Electronic properties of the yttriumdicarbide superconductors YC_2, $Y_{1-x}Th_xC_2$, $Y_{1-x}Ca_xC_2$ $(0<x\leqslant 0.3)$

Th. Gulden, R. W. Henn, O. Jepsen, R. K. Kremer, W. Schnelle, A. Simon, and C. Felser
Max-Planck-Institut für Festkörperforschung, Heisenbergstraße 1, D-70569 Stuttgart, Germany
(Received 16 May 1997)

We characterize the superconducting state of the carbides YC_2, $Y_{1-x}Th_xC_2$, and $Y_{1-x}Ca_xC_2$ $(0<x\leqslant 0.3)$ by means of magnetization and specific-heat measurements. YC_2 is a superconductor with $T_c=4.02(5)$ K. Partial substitution with Ca and Th, as well as doping with the strongly pair breaking Gd, reduces the critical temperature. Isothermal magnetization measurements on YC_2 indicate a superconducting behavior close to the type-I limit with $B_{c2}(0)=59(2)$ mT. Specific-heat data of YC_2, $Y_{0.8}Th_{0.2}C_2$, and $Y_{0.9}Ca_{0.1}C_2$ are analyzed in terms of weak-coupling BCS theory and the α model. The comparison with the model predictions as well as the $^{12}C/^{13}C$-isotope effect on T_c indicate excellent agreement with weak-coupling BCS theory for YC_2. A strong dependence of the superconducting properties on the carbon deficiency is observed. We describe high-temperature annealing procedures to optimize the superconducting properties of the samples. *Ab initio* calculations of the electronic band structure using the tight-binding linear muffin-tin orbital atomic-sphere approximation method are presented and the density of states at the Fermi energy is discussed in view of the experimental Pauli susceptibilities and heat-capacity results. [S0163-1829(97)06738-6]

I. INTRODUCTION

Interest in the properties of superconducting lanthanoid carbides has recently increased due to the discovery of superconductivity with transition temperatures up to 23 K in the Ni and Pd-based borocarbide families[1–3] and also because of the observation of superconductivity with T_c up to 11.6 K in layered rare-earth carbide halides.[4–7]

Binary and quasibinary lanthanoid (Ln) carbides, especially Th substituted sesquicarbides of yttrium and lanthanum, Ln_2C_3,[8] had attracted particular attention more than a decade prior to the discovery of superconducting cuprates because their transition temperatures reached values close to those of niobium based A15-type Nb_3X compounds.[9] Lanthanoid dicarbides LnC_2 (Ln=Y, La), which crystallize in the body-centered-tetragonal CaC_2 structure type[10] (see Fig. 1), exhibit lower transition temperatures. For example, Giorgi *et al.* detected superconductivity in YC_2 at 3.88 K.[11] Apart from reports on the appearance of superconductivity, however, to the best of our knowledge, further detailed investigations concerning the superconducting properties of YC_2 have not been carried out since.[12–14,8]

Stimulated by the interest in the layered yttrium-carbide-halide superconductors,[4–7] with crystal structures and chemical bonding properties closely related to those of the lanthanoid dicarbides,[15,16] we have carried out a detailed study of the superconducting properties of samples of YC_2, $Y_{1-x}Th_xC_2$, and $Y_{1-x}Ca_xC_2$ $(0<x\leqslant 0.3)$ by specific-heat and dc-magnetization measurements.[17] The analysis of the magnetization and specific-heat experiments as well as of the $^{12}C/^{13}C$-isotope effect on T_c of YC_2 reveals that these compounds behave as nearly ideal weak-coupling BCS superconductors. Th and Ca substitution reduces T_c, and the maximal T_c is therefore observed for compounds with the ideal composition of YC_2.

The electronic properties in the normal state have been studied by measuring the Pauli susceptibility and the specific heat of the conduction electrons. The experimentally determined electronic density of states at the Fermi energy is enhanced by Th substitution but lowered by Ca substitution.

Tight-binding linear muffin-tin orbital atomic-sphere approximation (TB-LMTO-ASA) calculations of the electronic band structure are presented and the electronic densities of states at the Fermi energy are discussed in view of the experimental results and electron-phonon coupling parameters are derived. Our investigations reveal a strong influence of the carbon deficiency on the superconducting properties of the yttrium dicarbides. Special high-temperature annealing procedures were employed to optimize the superconducting properties of our samples.

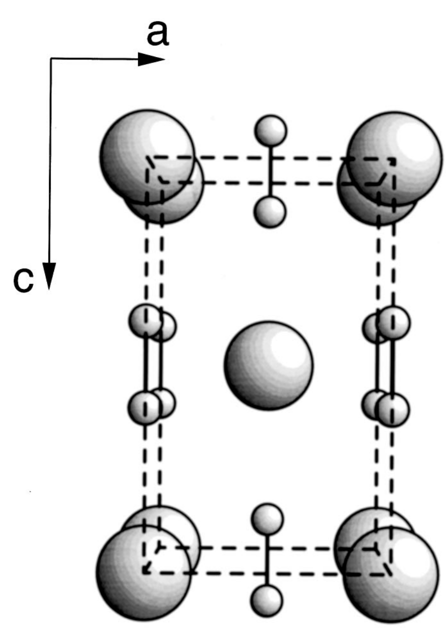

FIG. 1. Perspective view of the crystal structure of YC_2 along [010].

II. EXPERIMENTAL

A. Sample preparation

Pellets of about 1 g of YC_2 and the Th-substituted yttrium-dicarbides $(Y,Th)C_2$ were prepared by arc-melting stoichiometric quantities of coarse chips of yttrium metal (Johnson Matthey Inc., 99.99%), thorium metal (Goodfellow Inc., 99.5%) and graphite (Deutsche Carbone, 99.99%) in a purified argon atmosphere. ^{13}C (Chemotrade, enrichment 99%) was purchased in form of an amorphous powder. After melting the sample pellets were sealed in tantalum crucibles and annealed in an induction furnace to temperatures between 1200 and 2300 K.

CaC_2 was prepared from a mixture of distilled calcium (99.8%) and a slight excess of graphite powder. The thoroughly mixed powders were pressed into a tantalum crucible and heated to 1400 K. The Ca-substituted samples $Y_{1-x}Ca_xC_2$ ($x \leqslant 0.3$) were prepared by heating a pressed pellet of a mixture of appropriate amounts of powders of YC_2 and CaC_2 to 2000 K for several times followed by slow cooling to room temperature. Qualitative and quantitative chemical analysis confirmed the molar ratio of the constituents. X-ray powder diffraction proved single-phase samples which all crystallized in the body-centered-tetragonal CaC_2-structure type.[10]

B. Magnetization measurements

Measurements of the dc-magnetizations were performed with a superconducting quantum interference device magnetometer (MPMS, Quantum Design). The moisture sensitive samples were sealed in quartz glass sample tubes designed to give a negligible background signal. The sample tubes were filled with helium exchange gas to provide sufficient thermal contact. Diamagnetic shielding [zero-field cooled (zfc) susceptibility] and Meissner effect [field-cooled (fc) susceptibility] were measured in external magnetic fields of 1 mT.

The Pauli susceptibilities were determined from high-field ($1\ \mathrm{T} \leqslant \mu_0 H \leqslant 5\ \mathrm{T}$) susceptibility measurements applying the Honda-Owen extrapolation method[18] to correct for ferromagnetic impurities, a Curie-type correction for the susceptibility of paramagnetic impurities and the correction for closed-shell diamagnetism.

C. Specific-heat measurements

The heat capacities $c_p(T)$ were measured by a quasiadiabatic heat pulse method in a vacuum calorimeter. The samples were mounted onto a sapphire platform with a thin layer of Apiezon-N grease. Powder samples were sealed under 1 bar ^{4}He exchange gas into Duran capsules with a flat bottom face.

The heat capacities of the addenda (sample holder and Duran capsule) were determined in separate runs and subtracted. The absolute errors of the $c_p(T)$ data for YC_2 (sample 2a, 1.588 g) are of the order of 1% or better, while they are somewhat larger for the data of the powder samples.

III. ELECTRONIC STRUCTURE CALCULATIONS

The colorless insulating calcium carbide, CaC_2, can be considered as the prototype ionic carbide. Its structure contains C_2 units bonded via C≡C triple bonds ($d_{C-C}=120$ pm) in agreement with the formulation as $Ca^{2+}C_2^{2-}$. In a molecular view, all bonding p orbitals of the C_2 unit are filled and separated by a large energy gap from the empty, antibonding π^* and σ^* orbitals. The additional electron in YC_2 enters the lowest-lying π^* orbitals which, together with the Y d states, form the conduction band.[19–22]

TABLE I. Technical data concerning the band-structure calculations (see text).

	s	p	d	f	S (Bohr radii)
Y	l	i	l	i	3.743
C	l	l	i		1.412
$E1$	l	i			1.248
$E2$	l	i			0.845

The electronic structure of YC_2 was calculated *ab initio* using the self-consistent TB-LMTO-ASA method.[23] A local exchange-correlation potential was used[24] and all relativistic effects were included except for the spin-orbit coupling. The LMTO method has been described fully elsewhere[23,25] and we shall therefore only give some technical data of the calculations in Table I.

In this table the inclusion of a partial wave ($s\sim$ angular momentum 0, $p\sim 1$, and so on) in the LMTO basis set is indicated by an l (meaning low) and an included partial wave, which has been down folded is indicated by an i (meaning intermediate). S is the sphere radius in atomic units and $E1$ and $E2$ stand for interstitial spheres, which had to be inserted in order that the volume of all spheres in the unit cell equals the unit-cell volume. No overlap between two atomic centered spheres exceeded 16% and the overlap between an atomic sphere and an interstitial sphere did not exceed 18%. The interstitial spheres were located at the $\mathbf{a}/2 + \mathbf{c}/4$ and $0.2660\mathbf{b} + \mathbf{c}/3$ equivalent positions, respectively. The sphere radii and the positions of the interstitial spheres were determined by an automatic algorithm developed by Krier *et al.*[26] We used 1063 irreducible points in all tetrahedron $\mathbf{k}$-space integrations.[27]

The calculated electronic structure along some symmetry lines in the body-centered tetragonal Brillouin zone is shown in Fig. 2. The corresponding density of states is shown in Fig. 3 and is in qualitatively good agreement with that of Zhukov *et al.*[28] The energy bands may be understood using the orbital decoration technique.[29] The two lowest bands at around -14 and -6 eV ($E_F=0$ eV) are the bonding and antibonding combinations of the carbon s orbitals, respectively. The bonding combination of the two p_x and the two p_y orbitals form the two degenerate bands from Γ to Z around -3 eV, which split up in two bands away from this symmetry line. The fifth band at Z is due to the bonding combination of the two p_z orbitals. This hybridizes strongly with the higher lying Y d_{3z^2-1} orbitals and therefore contributes to the metal carbon bonding. All these bands are completely filled and they therefore contain 10 of the 11 valence electrons. The remaining electron is shared between the Y $d_{x^2-y^2}$ orbitals, which form a strongly dispersive band in planes perpendicular to the $\mathbf{c}$ direction with a small electron pocket around Z [$=(2\pi/a,0,0)$, not shown in Fig. 3], and combinations of Y d_{xz}, d_{yz}, antibonding C p_x, and anti-

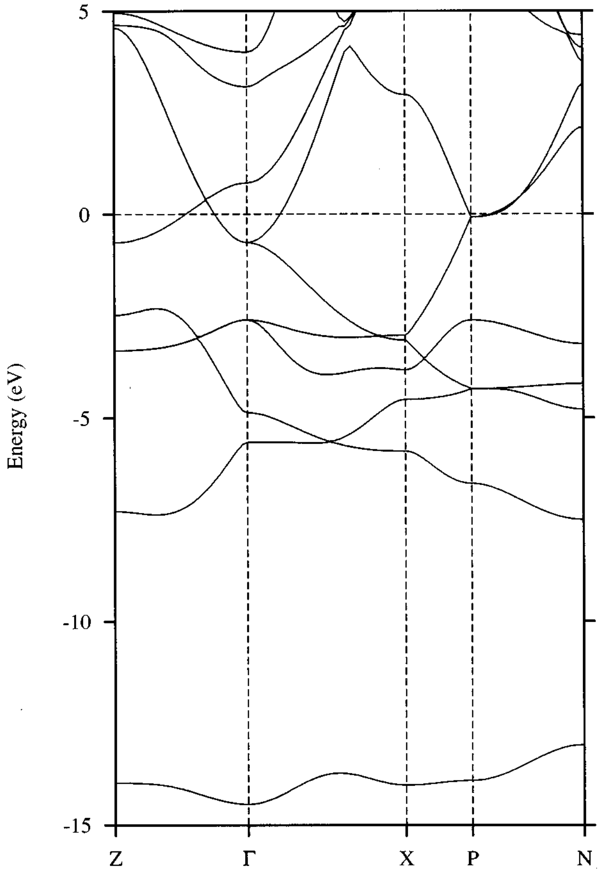

FIG. 2. Self-consistent energy band structure of YC_2 along some symmetry lines in the body-centered-tetragonal Brillouin zone. $Z=2\pi/c$ (0,0,1), $\Gamma=(0,0,0)$, $X=\pi/a$ (1,1,0), $P=\pi/a$ $(1,1,a/c)$, and $N=\pi/a$ $(1,0,a/c)$. The zero of energy is at the Fermi level.

bonding C p_y orbitals. The latter combination provides hopping between the YC_2 planes, and the corresponding bands consequently are strongly dispersive in the **c** direction. The density of states per formula unit at the Fermi level is $N(E_F)=0.34$ states eV^{-1} $spin^{-1}$. Using a rigid-band picture the densities for the thorium substituted compounds $Y_{1-x}Th_xC_2$ are estimated to be 0.35, 0.38, and 0.40 states eV^{-1} $spin^{-1}$ for x = 0.1, 0.2, and 0.3, respectively. The

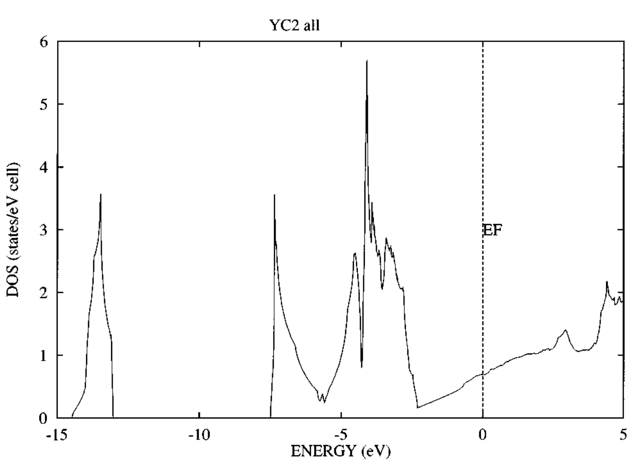

FIG. 3. Self-consistent total density of states of YC_2. The zero of the energy is at the Fermi level.

lattice expansion induced by Th substitution is very small, and it is estimated to reduce $N(E_F)$ by 0.7, 1.4, and 2.1 % for x = 0.1, 0.2, and 0.3, respectively. For the calcium-substituted compounds $Y_{1-x}Ca_xC_2$, $N(E_F)$ is calculated to be 0.34, 0.33, and 0.31 states eV^{-1} $spin^{-1}$ for x = 0.1, 0.2, and 0.3, respectively.

IV. RESULTS AND DISCUSSION

A. Sample characterization

Table II compiles the crystallographic and the superconducting properties of our samples. A central result of our investigation is the finding that the properties, and in particular the superconducting critical temperature, depend very sensitively on the carbon content of the samples. Proper heat treatment (see below) of the stoichiometric YC_2 samples results in superconductors with a sharp transition and transition temperatures up to 4.02 ± 0.05 K (onset temperature, sample $2a$). This temperature is somewhat higher than the T_c of 3.88 K reported previously for YC_2 by Giorgi *et al.*[11] The increased transition temperatures are observed only after heating the samples to 2300 K followed by a subsequent slow cooling to 1200 K at a rate of 50 K/h. For samples treated in this way the lattice parameters a and c are found to be largest. Rapid cooling, even of stoichiometric YC_2 samples, leads to a reduction of T_c to $\approx$ 3.86 K and a visible decrease of the lattice parameters, as well. We attribute this observation to local carbon defects which are induced by heating the samples to high temperatures and frozen in when subsequently quenching the samples from 2300 K to room temperature. The carbon excess is assumed to precipitate at the boundaries between YC_{2-x} grains.

Intentional reduction of the carbon content (samples 3 and 4) leads to a rapid, almost linear, decrease of T_c with the carbon deficiency, $\approx$ 0.1 K/% C (cf. Fig. 4), as well as a decrease of the lattice parameters, which is more pronounced for the c axis. The lattice parameters therefore are a sensitive indicator for the carbon content of the samples. The reduced carbon content, apparently, leads to a partial replacement of C_2 units by single C atoms as is also evidenced by a detailed investigation of the hydrolysis reaction of YC_{2-x} showing an increase of methane species in the hydrolysis products.[30,31]

A substitution of Y in YC_2 with Th or Ca results in compounds which, up to 30% substitution, still exhibit the CaC_2

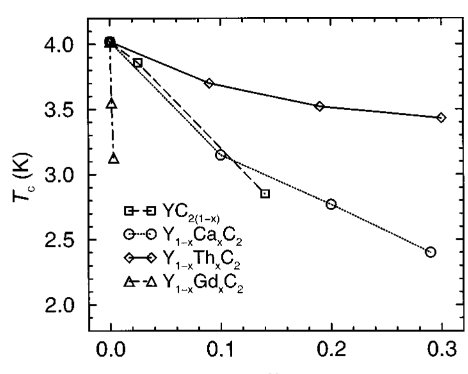

FIG. 4. T_c variation with C defects and Gd, Th, or Ca substitution of the cation Y.

TABLE II. Preparation conditions, lattice constants a and c, the superconducting transition temperature T_c (onset temperature of diamagnetic shielding) and the upper critical field B_{c2} of the investigated samples. A + sign in the column labeled ''slow cooled'' indicates that the sample was cooled down from 2300 to 1200 K at a rate of 50 K/h.

Sample	Composition	Preparation	Slow cooled	a (pm)	c (pm)	T_c (K)	B_{c2} (mT)
1	$Y^{13}C_2$	arc melting	+	366.35 (5)	617.86 (11)	3.85(5)	
2*a*	YC_2	arc melting	+	366.38 (3)	617.70 (8)	4.02(5)	
2*b*	YC_2	arc melting	+	366.44 (5)	617.62 (11)	3.98(4)	
2*c*	YC_2	arc melting	+			3.95(5)	59 (2)
2*d*	YC_2	arc melting	+			3.95(5)	60 (2)
3	$YC_{1.95}$	arc melting		366.37 (2)	617.32 (5)	3.86(5)	
4	$YC_{1.72}$	arc melting		365.43 (9)	611.51 (15)	2.85(10)	
5	$(Y_{0.91}Th_{0.09})C_2$	arc melting	+	367.72 (5)	619.38 (13)	3.70(5)	
6	$(Y_{0.81}Th_{0.19})C_2$	arc melting	+	369.18 (5)	621.19 (13)	3.52(5)	
7	$(Y_{0.70}Th_{0.30})C_2$	arc melting	+	370.56 (4)	623.21 (11)	3.43(5)	500 (50)
8	$(Y_{0.90}Ca_{0.10})C_2$	induction heating	+	368.04 (3)	619.27 (12)	3.15(8)	300 (50)
9	$(Y_{0.80}Ca_{0.20})C_2$	induction heating	+	368.44 (9)	619.89 (12)	2.82(10)	
10	$(Y_{0.71}Ca_{0.29})C_2$	induction heating	+	369.86 (9)	620.27 (17)	2.40(10)	

structure. The lattice parameters closely follow Vegard's law indicating a full assimilation of the dopants. All Th- or Ca-substituted samples consistently show lower superconducting transition temperatures in contrast to the Y_2C_3 system, where replacement of Y by Th leads to a significant increase of T_c.[8] Substitution of magnetic rare-earth atoms like, e.g., Gd for Y in YC_2, as well, induces a dramatic decrease of T_c (cf. Fig. 4).

The magnetic susceptibility measurements reveal a sharp transition to superconductivity with $\Delta T_c/T_c \approx$ 1–2 % for all samples. The diamagnetic shielding is complete while the Meissner-effect fraction typically is found between 10 and 70 %, depending on the annealing conditions (cf. Fig. 5).

B. Isotope effect

The shift of the superconducting transition temperature of YC_2 induced through the replacement of the natural mixture of C isotopes (98.9% ^{12}C) by isotopically enriched ^{13}C was studied on two samples which showed lattice parameters which within error bars were identical to those of the $Y^{12}C_2$ samples. The $^{12}C/^{13}C$ isotope effect on T_c of YC_2 amounts to (cf. inset Fig. 5)

$$\Delta T_c = -0.17(2)\ \ \text{K},$$

which corresponds to an isotope exponent of

$$\alpha = 0.51(7)$$

in very good agreement with the prediction of weak-coupling BCS theory.

C. Pauli susceptibility

Figure 6 displays the molar susceptibility $\chi_{mol}(T,\mu_0 H \to \infty)$ for $YC_{1.95}$ (sample 3) which is typical for all samples under investigation. Each data point was obtained from the extrapolation, $\mu_0 H \to \infty$, of a set of field-dependent magnetic-susceptibility measurements carried out at constant temperature (Honda-Owen method[18]).

Above 100 K the magnetic susceptibilities of all investigated samples can be fitted very well to a modified Curie law (see Fig. 6)

$$\chi_{mol} = C/T + \chi_0. \tag{1}$$

The Curie term C/T accounts for magnetic impurities which were found to amount to 0.25% or less of spin $S = 1/2$ entities per formula unit. The temperature-independent part, χ_0, represents the sum of the conduction electron paramagnetism (''Pauli susceptibility'') χ_{Pauli} and of the diamagnetism of the closed shells χ_{dia}:

$$\chi_0 = \chi_{Pauli} + \chi_{dia}. \tag{2}$$

χ_{dia} was calculated using the increments for the particular ions:[32] $Y^{3+}: -12\times10^{-6}$ emu mol^{-1}, $Ca^{2+}: -8 \times 10^{-6}$ emu mol^{-1}, and $Th^{4+}: -20\times10^{-6}$ emu mol^{-1}. For

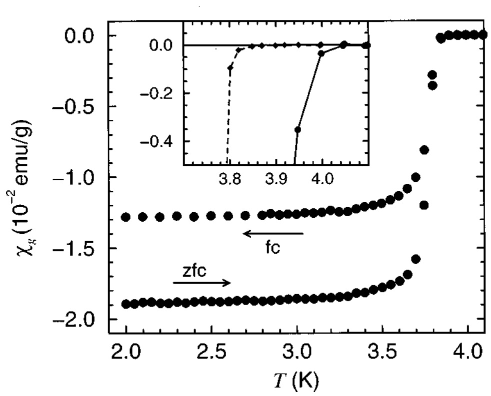

FIG. 5. Magnetic susceptibility of a well-crystallized sample of $YC_{1.95}$ (sample 3) which was annealed at 2300 K. Diamagnetic shielding (zfc) was measured after zero-field cooling and the Meissner effect (fc) by cooling in a field of 1 mT. The inset shows the onset of diamagnetic shielding (zfc susceptibility) for a sample of YC_2 (sample 2*a*) (●) and for $Y^{13}C_2$ (sample 1) (♦) on an enlarged scale.

TABLE III. Temperature-independent susceptibilities extracted from the fit of Eq. (1) to the experimental data. Diamagnetic susceptibilities, calculated Pauli susceptibilities and extracted density of states $N(E_F)_\chi$. An asterisk indicates that the measured temperature-independent susceptibility has been corrected for the diamagnetic susceptibility of the graphite impurities.

Sample	Composition	χ_0	χ_{dia}	χ_{Pauli}	$N(E_F)_\chi$	Graphite impurity
		(10^{-6} emu mol^{-1})			(eV^{-1} spin^{-1} f.u.$^{-1}$)	(mol %)
2*b*	YC_2	12.2(5)	−18.5	31	0.48	
2*c*	YC_2	14(1)*	−18.5	33	0.51	9.4
2*d*	YC_2	16(2)*	−18.5	33	0.53	15.6
3	$YC_{1.95}$	11.6(5)	−18.2	30	0.47	
5	$(Y_{0.91}Th_{0.09})C_2$	12.6(5)*	−19.5	32	0.50	2.6
6	$(Y_{0.81}Th_{0.19})C_2$	11.6(5)*	−20.6	32	0.50	2.9
7	$(Y_{0.70}Th_{0.30})C_2$	16.6(5)*	−21.8	38	0.58	1.2
8	$(Y_{0.90}Ca_{0.10})C_2$	1(1)	−18.1	19	0.30	

C_2^{3-} the increment was calculated according to Pascal's method to -6.5×10^{-6} emu mol^{-1}.[33] Samples 2*b*, 2*c*, 2*d*, 5, 6, and 7 (cf. Table III) were prepared with a slight surplus of carbon which we expect to precipitate in the preparation process as graphite impurities at grain boundaries. The graphite contribution to χ_{Pauli} was taken into consideration when evaluating the Pauli susceptibility by using a diamagnetic susceptibility of -90×10^{-6} emu mol^{-1} for polycrystalline graphite.[34]

From χ_{Pauli} the electronic density $N(E_F)_\chi$ at the Fermi energy E_F may be obtained from

$$N(E_F)_\chi=\chi_{Pauli}/2\mu_B^2. \quad (3)$$

The Pauli susceptibilities fall in a range of 19 to 38 $\times10^{-6}$ emu mol^{-1} for the different compounds and exhibit a clear dependence on the Th or Ca substitution with the tendency to increase with growing Th content and to decrease when replacing Y by Ca. This observation is in good agreement with the results of the band-structure calculations. Substitution with Th in the oxidation state 4+ raises the number of valence electrons per metal atom to values above 3 per metal atom, while Ca substitution (oxidation state 2+) reduces the valence electron count below 3. The TB-LMTO-ASA band-structure calculations show that the electronic density of states intersects the Fermi level with a positive slope (cf. Fig. 3). In a rigid-band model an increase of the number of valence electrons therefore is expected to raise the Fermi energy and to cause an increase of the electronic density of states and of χ_{Pauli}. Figure 7 displays the dependence of the Pauli susceptibility on the valence electron number per metal atom indicating the growth of χ_{Pauli} with that number, however with different slopes for the Ca- and Th-substituted samples. Interestingly, T_c is maximized for three valence electrons per metal atom and falls off when reducing or raising the number of valence electrons. The Pauli susceptibilities indicate a density of states at the Fermi level of about 0.5 eV^{-1} spin^{-1} f.u.$^{-1}$ which is about 50% larger than the values obtained from the band-structure calculations. This discrepancy indicates some exchange enhancement of the electronic susceptibility which will be discussed in detail below together with the Sommerfeld coefficients extracted from the low-temperature specific-heat measurements and the results of the band-structure calculations.

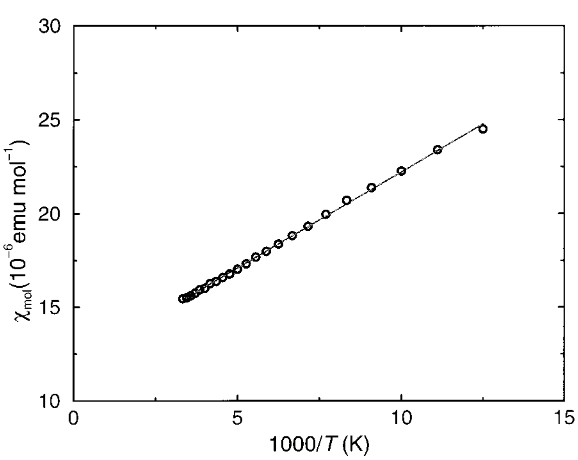

FIG. 6. Magnetic susceptibility of $YC_{1.95}$ (sample 3) between room temperature and 80 K. The fit with a modified Curie law [Eq. (1)] is indicated by the full line.

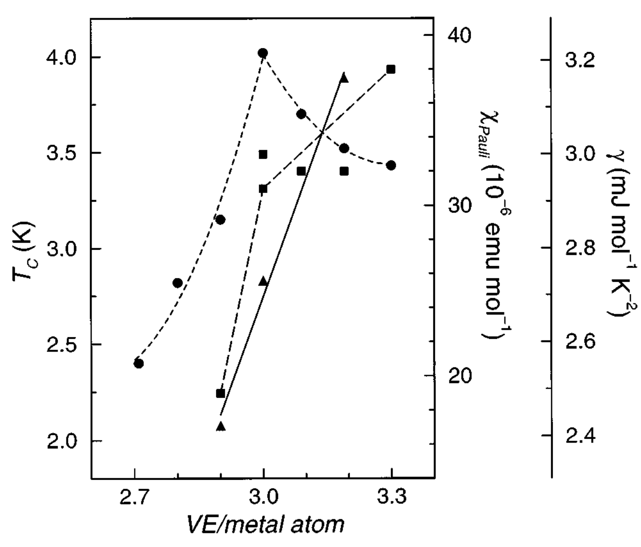

FIG. 7. Variation of T_c (●), the Pauli susceptibility χ_{Pauli} (■), and the Sommerfeld coefficient γ (▲) with the valence electron count (VE) per metal atom. Lines are guides for the eye.

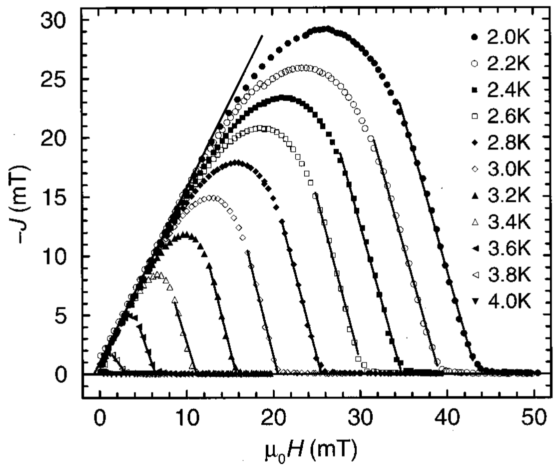

FIG. 8. Isothermal magnetic polarization $J(B)$ of a spherical sample of YC_2 (sample $2c$).

D. Magnetization

The isothermal magnetization was determined on a spherical sample of YC_2 $(2c)$. In Fig. 8 the negative polarization $-J(B)$ is plotted for temperatures between 2 and 4 K. The shape of these curves reflect the demagnetization due to the spherical sample geometry as is expected for a type-I superconductor with fully reversible magnetization. However, the polarization curves are irreversible once they deviated from the initial linear low-field increase. This behavior clearly indicates flux penetration in the Shubnikov phase of a type-II superconductor.

The analysis of the polarization curves within the scope of Ginzburg-Landau (GL) theory yields the characteristic lengths and critical fields. The GL parameter was determined from the slopes of the thermodynamic critical field ($B_{c\mathrm{th}}$) and the upper critical field (B_{c2}) near T_c (Fig. 9) according to

$$\kappa = \frac{1}{\sqrt{2}} \left(\frac{\partial B_{c2}/\partial T}{\partial B_{c\mathrm{th}}/\partial T} \right)_{T_c} \tag{4}$$

and amounts to $\kappa = 1.07(5)$. This value is close to the type-I–type-II limit of $1/\sqrt{2}$. The zero-temperature critical fields $B_{c2}(0) = 59(2)$ mT and $B_{c\mathrm{th}}(0) = 33(2)$ mT were calculated

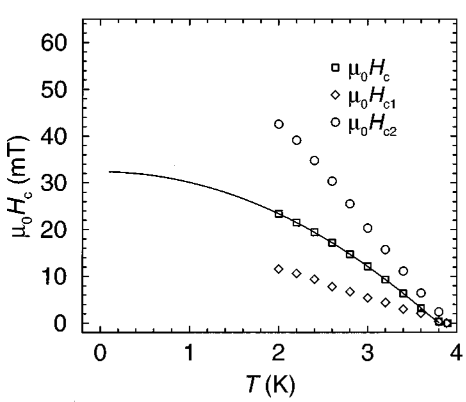

FIG. 9. Lower (B_{c1}), upper (B_{c2}), and thermodynamical ($B_{c\mathrm{th}}$) critical fields of YC_2 (sample $2c$). The full lines indicate a fit with a parabolic law.

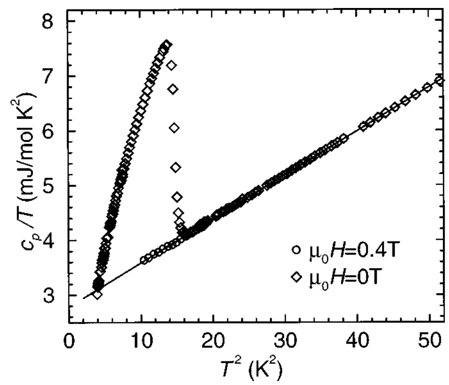

FIG. 10. Specific-heat capacity c_p/T vs T^2 of YC_2 (sample $2a$).

using BCS weak-coupling predictions. An upper limit for $B_{c1}(T)$ was estimated from the deviation of the $J(B)$ curves from the initial linear increase.

The coherence length and the penetration depth in the polycrystalline average amount to $\xi_{\mathrm{GL}}^{\mathrm{poly}} = 740(50)$ Å and $\lambda_{\mathrm{GL}}^{\mathrm{poly}} = 810(50)$ Å, respectively.

E. Specific heat

The specific-heat capacity of YC_2 (sample $2a$, bulk) is shown in Fig. 10 in a c_p/T vs T^2 representation. Data sets measured in zero field and in a field of 0.4 T are displayed. The lattice and electronic contribution of the normal-state specific heat $c_{p,N}$ up to $\approx$ 9 K are very precisely described by $c_{p,N}(T) = \gamma_N T + \beta T^3$ with $\gamma_N = 2.782(5)$ mJ/mol K^2 and β equivalent to an initial Debye temperature $\Theta_{\mathrm{D}}(0)$ of 418(1) K. The fit with the parameters γ and β is given in Fig. 10. The parameters of this and the following fits are listed in Table IV.

Figure 11 displays the difference Δc_p between the specific heats of the superconducting and the normal state ($\Delta c_p = c_{p,S} - c_{p,N}$) for sample $2a$. The difference Δc_p is fully described by the thermodynamic free enthalpy ΔG of a superconductor. The electronic specific heat $\Delta c_p(T/T_c)$ of a weak-coupling BCS-superconductor has been calculated by Mühlschlegel.[35] The jump at the transition $\Delta c_p(T_c)$ amounts to 1.4261 $\gamma_N T_c$.

In the upper panel of Fig. 11 we show a fit of this BCS model of the specific heat to our data of Δc_p. In order to model the data near the slightly smeared transition a Gaussian distribution of the transition temperatures was included. The parameters of the fit are T_c, the width of the transition $\Delta T_c/T_c$, and the electronic coefficient γ_S. We obtain $T_c = 3.840(1)$ K, $\Delta T_c/T_c = 0.77(3)\%$, and $\gamma_S = 2.790(5)$ mJ/mol K^2. The small transition width indicates good sample homogeneity, especially it indicates that there are only slight variations of the local carbon stoichiometry. A comparison of γ_S with γ_N shows excellent agreement (difference 0.3%). The plot, however, reveals small systematic differences of the BCS fit. The model predicts too low values in the range 0.82–0.95 T_c and too high values for $T < 0.82 T_c$.

A model for the thermodynamic properties of a superconductor with BCS-like Cooper pairing and variable electron-phonon coupling strength was suggested by Padamsee *et al.*[36] In this model (alpha-model) the ratio of the width of

TABLE IV. Parameters of the fits of models to the specific heat c_p of YC_2 in the normal-metallic ($B > B_{c2}$) and in the superconducting ($B=0$) state. BCS denotes a fit with a weak-coupling BCS model, α a fit with the α model.

Sample	Composition	Fit	T_c (K)	ΔT_c (%)	γ_S (mJ/mol K^2)	γ_N (mJ/mol K^2)	$\Theta_D(0)$ (K)
2a	YC_2	BCS	3.840(1)	0.77(03)	2.790(5)	2.782(5)	418
		$\alpha=1.82(1)$	3.83(2)	1.0(1)	2.67(1)	2.782(5)	418
2b	YC_2	BCS	3.825(8)	0.62(19)	2.73(4)		
6	$Y_{0.81}Th_{0.19}C_2$	BCS	3.585(5)	0.73(08)	3.19(3)	3.23(4)	368
		$\alpha=1.87(4)$	3.58(3)	1.1(1)	2.95(5)	3.23(4)	368
8	$Y_{0.90}Ca_{0.10}C_2$	BCS	2.994(7)	1.0(2)	2.43(4)	2.82(2)	427
		$\alpha=1.83(2)$	3.00(1)	1.5(2)	2.40(4)	2.82(2)	427

the gap at the Fermi level at zero temperature $\alpha = \Delta(0)/k_B T_c$ is used to parametrize the specific heat Δc_p. In the lower panel of Fig. 11 we display a fit with this model. The free parameters are T_c, $\Delta T_c/T_c$, γ_S, and α. We obtain values for T_c and $\Delta T_c/T_c$ very similar to those of the BCS model, while the γ_S is slightly smaller [2.67(1) mJ/mol K^2]. The ratio of γ_S/γ_N deviated now 4% from unity. For the gap parameter we find $\alpha = 1.82(1)$; a value very close to the weak-coupling BCS limit of $\alpha_{BCS}=1.764$.

The specific heats of a sample in which 20% of the yttrium has been substituted by thorium ($Y_{0.8}Th_{0.2}C_2$, sample 6), and of a 10% calcium substituted sample ($Y_{0.9}Ca_{0.1}C_2$, sample 8) are shown in Fig. 12 again in a $\Delta c_p(T)$ representation. As described above, both substitutions lower T_c. The effect on the electronic specific heat, however, is different. While the coefficient γ_N for the Th-substituted sample is increased by 16% with respect to the value for YC_2, the γ_N of the Ca-substituted sample is, within error, the same as in the unsubstituted compound. The parameters for the fits on these two samples are also given in Table IV.

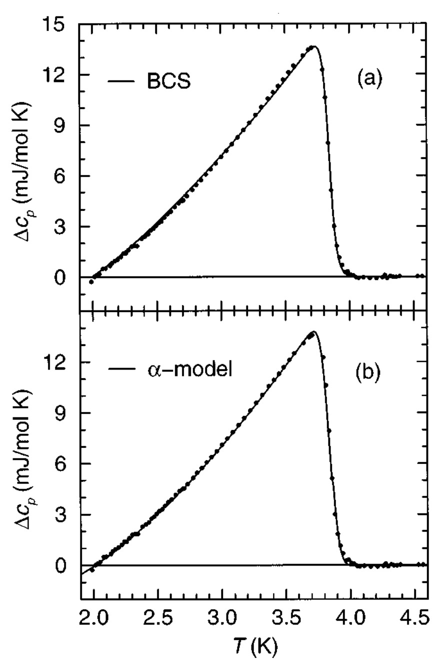

FIG. 11. Difference $\Delta c_p(T)$ of the specific heats of YC_2 (sample 2a) in the superconducting and the normal state. Fits of the BCS model and the α model are given by the full lines (details see text).

The initial Debye temperatures $\Theta_D(0)$ for the Th- and the Ca-substituted sample are 368 and 427 K, respectively. They are in good accordance with the values calculated from a scaling of $\Theta_D(0) = 418$ K of YC_2 with the ratio $\sqrt{M_{YC_2}/M_{(Y,Th,Ca)C_2}}$ of the molar masses, M, of the individual compounds.

A fit of the α model to the data of the Th- and Ca-substituted samples (6 and 8) reveals a slightly enhanced parameter α indicating a tendency to an increased electron-phonon coupling. However, the quality of the $\Delta c_p(T)$ data of these samples is not sufficient to unambiguously distinguish the BCS fit from the α fit (cf. Table IV). The Sommerfeld coefficients extracted from these fits nicely follow a linear relationship over the valence electron count (cf. Fig. 7) which is similar to the Pauli susceptibilities.

F. Electronic properties

In this section we discuss relevant electronic parameters as they can be derived from the results of the specific heat and susceptibility measurements.

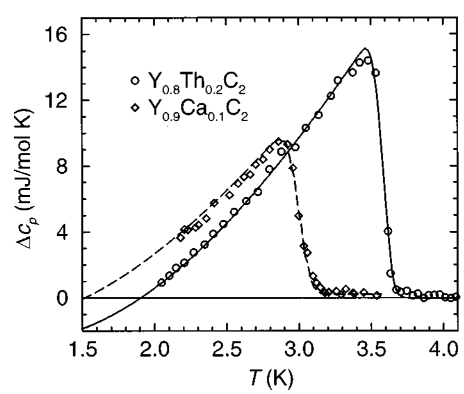

FIG. 12. Difference $\Delta c_p(T)$ of the specific heats of $Y_{0.81}Th_{0.19}C_2$ and $Y_{0.90}Ca_{0.10}C_2$ (samples 6 and 8, respectively) in the superconducting and the normal state. Fits of the α model are given by the lines (details see text).

TABLE V. Compilation of the density of states at the Fermi energy as calculated from the band-structure calculations $[N(E_F)_{BS}]$, from the Pauli susceptibilities $[N(E_F)_\chi]$ and from the measured electronic specific heat $[N(E_F)_{\gamma_{exp}}]$. λ_{tot} represents the total enhancement of the electronic specific heat [see Eq. (4)], λ_{MM} is the electron-phonon coupling constant calculated from the McMillan equation, and U the Stoner enhancement factor.

Composition	$N(E_F)_{BS}$ (eV^{-1} spin^{-1} f.u.$^{-1}$)	$N(E_F)_{\gamma_{exp}}$	$N(E_F)_\chi$	λ_{tot}	λ_{MM}	U
$(Y_{0.81}Th_{0.19})C_2$	0.38	0.67	0.50	0.76	0.51	0.24
YC_2	0.34	0.58	0.50	0.71	0.55	0.32
$(Y_{0.90}Ca_{0.10})C_2$	0.34	0.51	0.29	0.50	0.52	≈ 0

The electronic specific heat may be enhanced over its bare value by electron-phonon coupling and by electronic correlations. The enhancement factor λ_{tot} contains the total mass enhancement due to both contributions and is defined by

$$\gamma_{exp} = (1+\lambda_{tot})\gamma_{BS} \tag{5}$$

with γ_{BS} being the ''bare'' Sommerfeld coefficient which is related to the calculated electronic density of states $N(E_F)_{BS}$ at the Fermi energy via

$$\gamma = \frac{2}{3}\pi^2 k_B^2 N(E_F)_{BS}. \tag{6}$$

Using the McMillan equation an estimate of the electron-phonon coupling parameter λ_{MM} from the measured critical temperatures T_c and the Debye temperatures can be made.[37] With a pseudopotential $\mu^* \approx 0.13$ we arrive at electron-phonon coupling parameters of about 0.5 and almost no variation over the three investigated samples. All results are compiled in Table V together with the density of states obtained from the TB-LMTO-ASA band-structure calculations and the density of states $N(E_F)_\chi$ calculated from the Pauli susceptibilities according to Eq. (3).

The enhancement factor λ_{tot} is about 40% larger than the electron-phonon coupling constants estimated from the McMillan equation pointing to some enhancement by electronic correlations. Enhancement by electronic correlations is as well indicated by the Stoner parameter U which was deduced from the comparison of the experimental Pauli susceptibilities and the bare Pauli susceptibilities calculated from the TB-LMTO density of states according to Eq. (3)

$$\chi_{Pauli}^{exp} = \chi_{Pauli}/(1-U). \tag{7}$$

In contrast to the behavior of λ_{MM}, λ_{tot}, and U vary with the number of valence electrons donated by the metal atoms to the C_2 units. λ_{tot} increases with increasing number of valence electrons while U shows a maximum at YC_2 like the superconducting transition temperature. The origin of this behavior is not clear at present.

Finally, we briefly discuss the variation of T_c induced by substitution of Ca or Th which both lead to a decrease of T_c. The reduction of T_c induced by Th substitution clearly contrasts the behavior of yttrium sesquicarbide, $Y_{2-x}Th_xC_3$ where a maximum T_c of 17 K for a formal charge -4.5 of the C_2 unit is reached for the compound $Y_{0.7}Th_{0.3}C_{1.55}$.[13,39]

It is particularly interesting to note, that the reduction of T_c is significantly more pronounced in case of Ca than in case of Th substitution (cf. Fig. 7). A clue to understand this difference may come from our findings in the layered $Y_2Br_2C_2$ system.[38] Intercalation of Na *between* the layers leading to the injection of electrons into the layers is accompanied by an increase of T_c. An equivalent addition of electrons due to a substitution of Y by Th *inside* the layers, however, leads to a decrease of T_c. The expected increase of T_c through raising the Fermi level, apparently, is overcompensated by a decrease of T_c through introducing disorder inside the layers in the latter case. The substitution of Y by Th in YC_2 results in a similar decrease of T_c which, however, is less pronounced than in case of Ca substitution where both the decrease of the Fermi level and disorder lower T_c. Obviously, substitution of C_2 units by single C atoms (replacement of C_2^{3-} by C^{4-}) introduces rather similar changes to the system as replacing Y^{3+} by Ca^{2+} causing a rather identical response of the system with respect to T_c (cf. Fig. 4).

V. SUMMARY AND CONCLUSIONS

In summary, the compound YC_2 and its Th/Ca-substituted variants represent a set of interesting superconductors. The results of our extensive experiments unambiguously prove bulk superconductivity in all investigated compounds. The modeling of the thermodynamic properties reveals almost ideal BCS-type behavior in the weak-coupling limit. The carbon isotope effect on the T_c investigated for the compound YC_2 is in best agreement with this conclusion. The analysis of the magnetization curves yields Ginzburg-Landau parameters slightly above the limit of $1/\sqrt{2}$ (type-II superconductor).

Most intriguing are the results of the Th- and Ca-substitution experiments: While the Sommerfeld coefficients of the electronic specific heat, the Pauli susceptibilities, and the Debye temperatures show a monotonic behavior as function of the electron concentration, T_c exhibits an extremum. The maximum transition temperature in the system $(Y,Th/Ca)C_2$ is observed close to a valence electron number of 3 per metal atom viz. for the stochiometric compound YC_2. We ascribe the appearance of this maximum to a complex interplay of the degree of electronic filling and disorder due to the substitution of Y with Ca and Th atoms.

ACKNOWLEDGMENTS

We thank E. Brücher, R. Eger, C. Hochrathner, K. Ripka, and N. Rollbühler for experimental assistance. Valuable discussions with E. Gmelin, Hj. Mattausch, and E. H. Brandt are gratefully acknowledged.

[1] R. Nagarajan, C. Mazumdar, Z. Hossain, S. K. Dhar, K. V. Gopalakrishnan, L. C. Gupta, C. Godart, B. D. Padalia, and R. Vijayaraghavan, Phys. Rev. Lett. **72**, 274 (1994).
[2] R. J. Cava, H. Takagi, B. Batlogg, H. W. Zandbergen, J. J. Krajewski, W. F. Peck, Jr., R. B. van Dover, R. J. Felder, T. Siegrist, K. Mizushashi, J. O. Lee, H. Eisaki, S. A. Carter, and S. Uchida, Nature (London) **367**, 146 (1994).
[3] R. J. Cava, H. Takagi, H. W. Zandbergen, J. J. Krajewski, W. F. Peck, Jr., T. Siegrist, B. Batlogg, R. B. van Dover, R. J. Felder, K. Mizuhashi, J. O. Lee, H. Eisaki, and S. Uchida, Nature (London) **367**, 252 (1994).
[4] A. Simon, Hj. Mattausch, R. Eger, and R. K. Kremer, Angew. Chem. Int. Ed. Engl. **103**, 1210 (1991).
[5] A. Simon, A. Yoshiasa, M. Bäcker, R. W. Henn, R. K. Kremer, Hj. Mattausch, and C. Felser, Z. Anorg. Allg. Chem. **622**, 123 (1996).
[6] R. W. Henn, W. Schnelle, R. K. Kremer, and A. Simon, Phys. Rev. Lett. **77**, 374 (1996).
[7] R. W. Henn, Ph.D. thesis, Universität Karlsruhe (TH), 1996.
[8] M. C. Krupka, A. L. Giorgi, N. H. Krikorian, and E. G. Szklarz, J. Less-Common Met. **19**, 113 (1969).
[9] See, e.g., *Superconductivity*, edited by R. Flükiger and W. Klose, Landolt-Börnstein, New Series Group III, Vol. 21 (Springer-Verlag, Berlin, 1990).
[10] M. Atoji, J. Chem. Phys. **35/6**, 1950 (1961).
[11] A. L. Giorgi, A. L. Szklarz, M. C. Krupka, T. C. Wallace, and N. H. Krikorian, J. Less-Common Met. **14**, 247 (1968).
[12] T. Sakai, Gin-Ya Adachi, T. Yoshida, and J. Shiokawa, J. Less-Common Met. **8**, 91 (1981).
[13] B. Cort, G. R. Stewart, and A. L. Giorgi, J. Low Temp. Phys. **54**, 149 (1984).
[14] R. W. Green, E. O. Thorland, J. Croat, and S. Legvold, J. Appl. Phys. **40**, 3161 (1969).
[15] U. Schwanitz-Schüller and A. Simon, Z. Naturforsch. B **40**, 7 (1985).
[16] Hj. Mattausch, R. K. Kremer, R. Eger, and A. Simon, Z. Anorg. Allg. Chem. **609**, 7 (1992).
[17] Th. Gulden, Ph.D. thesis, Universität Stuttgart, 1997.
[18] K. Honda, Ann. Phys. (Leipzig) **32**, 1027 (1910); M. Owen, *ibid.* **37**, 657 (1910).
[19] J. R. Long, R. Hoffman, and H.-J. Meyer, Inorg. Chem. **31**, 1734 (1992).
[20] J. R. Long, J.-F. Halet, R. Hoffman, H.-J. Meyer, and J.-Y. Saillard, New J. Chem. **16**, 839 (1992).
[21] G. J. Miller, J. Am. Chem. Soc. **116**, 6332 (1994).
[22] E. Ruiz and P. Alemany, J. Phys. Chem. **99**, 3114 (1995).
[23] O. K. Andersen, Phys. Rev. B 12, 3060 (1975); O. K. Andersen and O. Jepsen, Phys. Rev. Lett. **53**, 2571 (1984).
[24] U. von Barth and L. Hedin, J. Phys. C **4**, 2064 (1971).
[25] O. K. Andersen, O. Jepsen, and D. Glötzel, in *Highlights of Condensed-Matter Theory*, edited by F. Bassani, F. Fumi, and M. P. Tosi (North-Holland, New York, 1985).
[26] G. Krier, O. Jepsen, and O. K. Andersen (unpublished).
[27] O. Jepsen and O. K. Andersen, Solid State Commun. **9**, 1763 (1971); P. E. Blöchl, O. Jepsen, and O. K. Andersen, Phys. Rev. B **49**, 16 223 (1994).
[28] V. P. Zhukov, N. I. Medvedeva, D. L. Novikov, and V. A. Gubanov, Phys. Status Solidi B **149**, 175 (1988).
[29] O. Jepsen and O. K. Andersen, Z. Phys. B **97**, 35 (1995).
[30] T. Y. Kosolapova, G. N. Makarenko, and L. T. Domasevich, in *Refractory Carbides*, edited by V. S. Samsonov (Consultants Bureau, New York, 1974), p. 417.
[31] Y. B. Paderno, V. L. Yupko, B. M. Rud, and G. N. Makarenko, Inorg. Mater. **2**, 540 (1966).
[32] P. W. Selwood, *Magnetochemistry* (Interscience, New York, 1956).
[33] R. R. Gupta, *Diamagnetic Susceptibility*, edited by K.-H. Hellwege and A. M. Hellwege, Landolt-Börnstein, New Series Group II, Vol. 16 (Springer-Verlag, Berlin, 1986).
[34] N. Ganguli and K. S. Krishnan, Proc. R. Soc. London **117**, 168 (1941); H. T. Pinnick and P. Kiive, Phys. Rev. **102**, 58 (1956).
[35] B. Mühlschlegel, Z. Phys. **155**, 313 (1959).
[36] H. Padamsee, J. E. Neighbor, and C. A. Schiffman, J. Low Temp. Phys. **12**, 387 (1973).
[37] W. L. McMillan, Phys. Rev. **167**, 31 (1968).
[38] M. Bäcker, A. Simon, R. K. Kremer, Hj. Mattausch, R. Dronskowski, and J. Rouxel, Angew. Chem. **108**, 837 (1996); Angew. Chem. Int. Ed. Engl. **35**, 752 (1996).
[39] For a compilation of the literature data, cf. A. Simon, J. Alloys Compd. **229**, 158 (1995).